Fibers and Polymers 2021, Vol.22, No.6, 1711-1717
DOI 10.1007/s12221-021-0871-7

ISSN 1229-9197 (print version)
ISSN 1875-0052 (electronic version)

Color Changes in Some UV Irradiated Polymer Nanocomposite Materials for the Application in Textile Industry

S. A. Nouh[1,2]*, M. ME. Barakat[3,4], Huda A. El-Nabarawy[5], K. Benthami[6], and N. Elhalawany[7]

[1]*Physics Department, Faculty of Science, Taibah University, Al-Madina al Munawarah, B.P 44256, Saudi Arabia*
[2]*Physics Department, Faculty of Science, Ain Shams University, Cairo, B.P 11865, Egypt*
[3]*Physics Department, Faculty of Science Yanbu, Taibah University, Yanbu, B.P 41912, Saudi Arabia*
[4]*Physics Department, Faculty of Science, Alexandria University, Alexandria, B.P 21500, Egypt*
[5]*Clothes and Jewelry Design Department, College of Family Science, Taibah University, Al-Madina al Munawarah, B.P 44256, Saudi Arabia*
[6]*Physics Department, Faculty of Science, University of Moulay Ismail, Meknes, B.P 11201, Morocco*
[7]*Polymers and Pigments Department, National Research Center, Cairo, B.P 11865, Egypt*
(Received July 23, 2020; Revised August 5, 2020; Accepted September 6, 2020)

Abstract: Four nanocomposites (NCPs), e.g., polyaniline-copper/polymethyl methacrylate (PANI-Cu/PMMA), polyaniline-copper/cellulose triacetate (PANI-Cu/CTA), polyaniline-copper/polycarbonate (PANI-Cu/PC), and polyaniline-copper/ polycarbonate-polyester (PANI-Cu/PC-PBT) were fabricated using both chemical oxidation and casting techniques. The morphology of the prepared NCPs was studied using scanning electron microscopy. The induced alterations in the color of the synthesized NCPs owing to UV irradiation, within fluences 25-120 J/cm^2, have been illustrated via UV spectroscopy and CIE color divergence methodology. The color variation between the pristine and irradiated NCP samples (color intensity, ΔE) has been computed for the four NCPs. The results show that, upon UV irradiation up to 120 J/cm^2, the values of ΔE for the PANI-Cu/PMMA NCP samples achieved a major color difference which is an acceptable match in commercial reproduction on printing presses since ΔE reached the value of 35.8. The value of ΔE for the PANI-Cu/CTA NCP samples reached 23.8 that also indicates a significant color difference. It is worth mentioning that the PANI-Cu/PC-PBT shows a minimum color difference since ΔE exhibited variation up to 7. This means that the PANI-Cu/PC-PBT NCP samples have higher resistance to color changes against UV radiation. Thus, this NCP may be a suitable candidate in textile industry.

Keywords: Polymers, Nanocomposites, Color changes, Radiation, UV spectroscopy

Introduction

Some polymers that are used in industry have various attractive characteristics that permit it to be most significant polymers. In spite of their huge technological and financial importance, however, they still have many problems owing to their narrow absorption bands and degradation mechanism that cause variation in their color properties [1]. This can be owing to the structure defects created throughout the polymerization route [2]. These problems can be solved by implementing nanoparticles (NPs) inside their matrices due to their small size that enhances the polymer properties [3]. The optical properties of the resulted polymeric nanocomposites (NCPs) display an essential role in research due to their great presentation in numerous industrial applications [4-6].

Polyaniline (PANI) is a talented conducting polymer for the electronic applications due to its environmental stability [7]. It is useful in textiles industry [8]. PANI which is used as a strain sensor has received awareness lately [9,10]. The high aromatic structure of PANI allows its backbone to be rigid. In spite of this, PANI is accessible in rather low molecular weight structure, thus its solution elasticity is usually inadequate to be electro-spun directly into fibers [11]. This character confines its application. Therefore, blending PANI with other polymers that have good mechanical and processing properties is a useful route.

Also, polymethyl methacrylate (PMMA) optical fiber, has been wicker with cotton and polyester in a specific weave pattern to evaluate the light for light releasing textile application. The illumination of clothing scheme is mainly affected by the weave geometry. The chance of mixing of PMMA with clothing scheme has been illustrated widely [12]. Although PMMA is distinguished between polymeric materials, it can't be suitable candidate for applications requiring high temperature due to its relatively poor thermal stability [13]. This can be treated by introducing nanoparticle effect [14]. Thus the PANI/PMMA blend combines the superior property of PMMA and the great electrical conductance of PANI, presenting brilliant strain and gas sensing property [15].

Besides, cellulose triacetate (CTA) is a good host material for PANI NCPs and has the advantages of transparent film formation. Numerous researches focusing on the physical properties of PANI and CTA blends have been reported [16,17]. CTA is used in numerous textile applications owing to its quality and excellent textile processing presentation. It is used in wicker fabrics, knits, and braids. It is regularly blended with other fibers to produce mixture threads [18].

*Corresponding author: samin273@gmail.com

Additionally, polycarbonate (PC) has significant characteristics such as good toughness; inflexibility and being thermally stable [19]. PC is amongst the most chemically resistant and durable polymers that can be bonded to the textile as a multi-layered coating; significantly enhancing the lifetime of the fabric through its resistance to bleach and other cleaning agents. PC is an appropriate matter for hosting metal NPs owing to its unique properties. The inclusion of metal NPS into the PC matrix has a benefit because the merged matter joins the properties from both materials [20-22].

Moreover, polyester (polybutylene terephthalate PBT) is semicrystalline which is chemically stable. Blend of polyester with polycarbonate is a category of industrial blends which can be applied. The product would be of enhanced chemical resistance and the flow properties [19]. The transesterification is the mainly essential substitute reaction between PC and PBT, resultant in a novel chemical construction of copolymers [19].

On the other hand, the color difference due to irradiation is an important procedure that evaluates the structural changes in polymeric nanocomposites. This procedure initiates the foundations which consider the construction of radiation sensors [23]. Several studies have considered the calculation of the color divergence in irradiated polymeric materials and the application in dosimetry [24-26]. Scientists have attributed the color modifications in irradiated polymers to the creation of hot free radicals and strongly conjugated bonds [27]. The UV irradiation treatment of polymeric materials causes rupture of bonds, production of free radicals and consequently, crosslinking is achieved [28]. Additionally, it creates significant lattice defects that lead to the formation of reactive species which can alter the optical properties of the irradiated polymeric materials [29]. The effectiveness of these modifications is based on the structure of the polymeric materials [30]. In our previous work, we prepared PANI-Mn/PMMA NCP as a γ-ray dosimeter. We found that the prepared NCP undergo color variations upon γ-irradiation [31]. In the present study, PMMA, CTA, PC, and PC-PBT were used as host materials to PANI-Cu NCP. The presence of Cu NPs is solely to encourage the charge transfer process due to the shift of charge density between molecular orbital of Cu NPs and those of PANI which are ligand in character [32].

The modifications of color in the synthesized NCP samples upon UV irradiation have been explored. The aim is to obtain a NCP of high resistance to color changes upon UV irradiation, improving its performance in textiles industry.

Experimental

Materials

Aniline monomer, dodecyl benzene sulfonic acid (DBSA, surfactant), copper chloride, and PMMA powder were obtained from Sigma-Aldrich Company, USA. CTA sheets were manufactured by Eastman Kodak Company, Rochester, New York. Bisphenol-A PC and bisphenol-A PC blended with polyester (PC-PBT blend-film) were produced by Farbenfabriken Bayer A.G., Leverkusen (West Germany).

Syntheses of PANI

A stable polyaniline-dodecylbenzenesulfonic acid (PANI-DBSA) colloidal dispersion was prepared as previously published [32] as follows: aniline monomer and dodecyl benzene sulfonic acid (DBSA) of ratio (3:1) in 75 m*l* water/isopropanol (IPA) mixture (3:1) have been homogenized for 10 min to form the miniemulsion. Then, 25 m*l* of ammonium peroxydisulfate (APS) solution (1 wt.%) was added dropwisely to the former miniemulsion. Polymerization was performed, at room temperature, with strong stirring at 10,000 rpm for 15 min. The color was changed from white anilinium-DBSA complex in water to blue, then turned into dark green. Finally, a green and very stable PANI-DBSA dispersion was obtained. The colloid dispersal is centrifuged, washed by water/methanol mix for several times and then dried in an electric oven for 4 h at 70 ^{o}C and kept for further use.

Syntheses of PANI-Cu NCP

The polymerization reaction has been done; where aniline monomer and DBSA of ratio (3:1) was homogenized by high shearing affect homogenizer at 10,000 rpm in existence of DBSA to form the miniemulsion. A 20 m*l* of 0.25 % copper chloride solution has been added to the formed miniemulsion with continuous strong stirring at 10,000 rpm until a green colloidal dispersion of PANI/Co NCP is obtained. The produced green colloidal dispersion was then centrifuged, washed several time by water/methanol mix, filtered, and dried at 70 °C for 4 h [32].

Syntheses of PANI-Cu/PC NCP

3 g of PC powder were dropwisely added to 50 m*l* of DMF with a continuous vigorous stirring until all PC powder liquefies. Then 0.125 g of the prepared PANI/Co was added to the preceding solution under stirring at room temperature until a homogeneous colored solution is obtained. The obtained solution was then casted onto clean Petri dish and left to dry at 50 ^{o}C for 24 h. The same has been done to prepare PANI-Cu/PMMA, PANI-Cu/CTA, and PANI-Cu/PC-PBT.

Irradiation Facilities

These NCP samples were irradiated with UV light in the fluence range 25-120 kJ/cm^2. A Hg lamp of 50 W, at 50/60 Hz, with an illumination flux of 3.14 W/cm^2, was used.

Instrumentation

The morphology of the synthesized NCPs samples was investigated using scanning electron microscope (JEOL, JSM-5910LV).

The UV spectroscopic analysis was performed with UV-Vis spectrophotometer (Jasco 570, 370-780 nm). The color of samples was studied by applying the CIE method. The CIELAB color intensity was calculated following previous route [33]:

$$\Delta E = [(L_1^* - L_2^*)^2 + (a_1^* - a_2^*)^2 + (b_1^* - b_2^*)^2]^{1/2} \quad (1)$$

where the subscripts 1 and 2 refer to the irradiated and non irradiated samples.

Results and Discussion

SEM Analysis for the Synthesized NCPs

Figure 1(a) shows the SEM image of the synthesized PANI-Cu NCP. It is seen that the Cu NPs are well dispersed into PANI matrix and are in the range from 80-85 nm in size. One can conclude that the formed NPs are in the range of nanosize and represented as bright spots or zones which are quite embedded into the darker zones of PANI matrix.

Figures 1(b)-(e) show the SEM images of the PANI-Cu/PMMA, PANI-Cu/CTA, PANI-Cu/PC, and PANI-Cu/PC-PBT NCPs, respectively. It is shown that the PANI/Cu is well dispersed and compatible with the four polymer matrices. The bright spots are for the Cu NPs.

Color Changes in the UV Irradiated PANI-Cu/PMMA NCP Samples

The transmission spectra of the pristine and UV irradiated PANI-Cu/PMMA, in the wavelength range 370-780 nm are shown in Figure 2. The real red, green, and blue lights are replaced by mathematical lights set, *X*, *Y*, and *Z* called

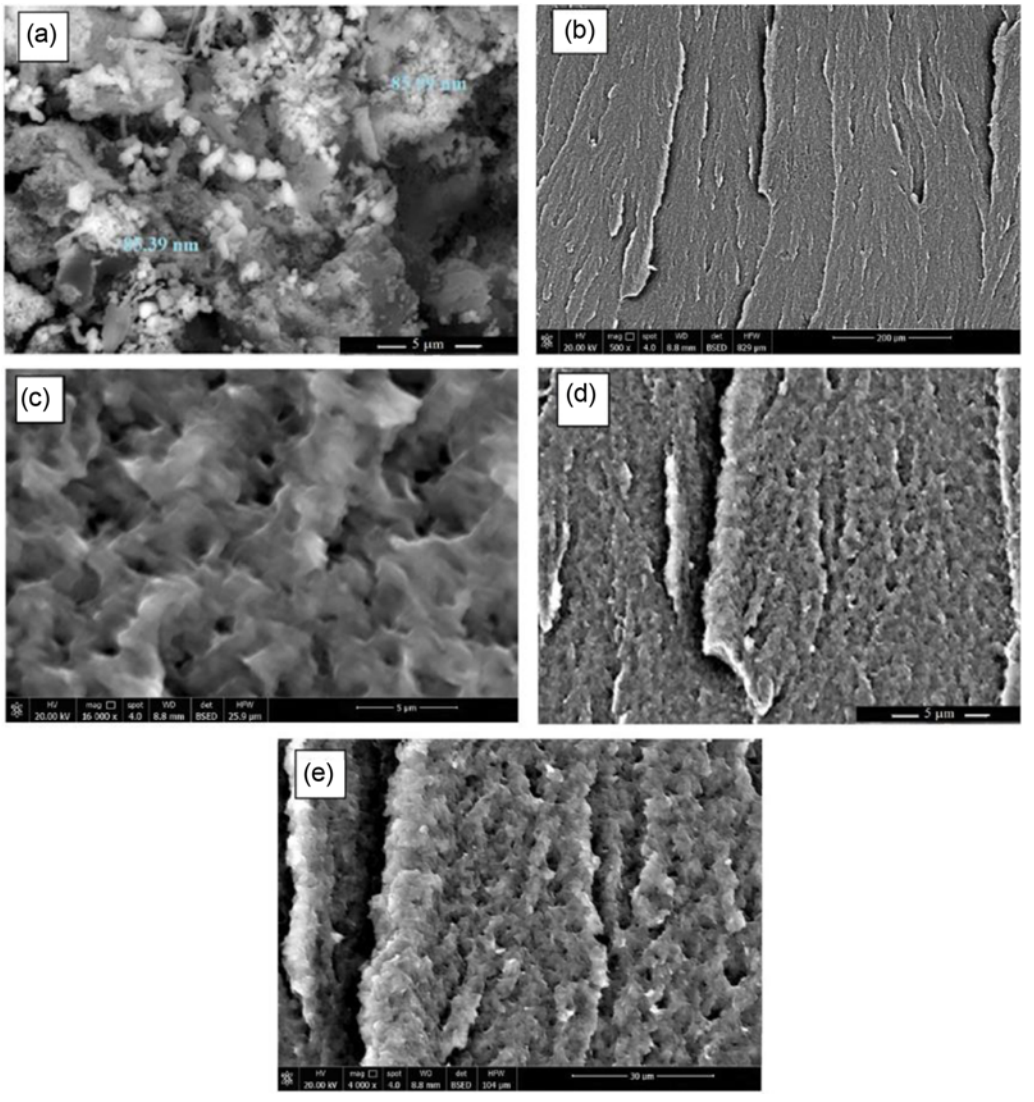

Figure 1. SEM micrographs of the pristine (a) PANI/Cu, (b) PANI-Cu/PMMA, (c) PANI-Cu/CTA, (d) PANI-Cu/PC, and (e) PANI-Cu/PC-PBT NCP samples.

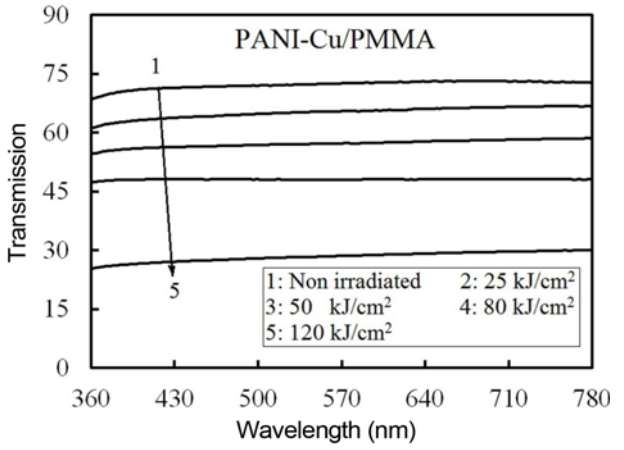

Figure 2. UV-Vis transmission spectra, in the 370-780 nm range, of the pristine and UV irradiated PANI-Cu/PMMA NCP samples.

tristimulus values [34]. The CIE tristimulus values for a sample are calculated by adding the product of the spectral power distribution of illuminant, the transmittance factor of the sample, and the color matching functions of the observer at each wavelength of the visible spectrum as illustrated before [34]. The tristimulus values and chromaticity coordinates were computed by means of the transmittance values at the wavelength range 370-780 nm. Their dependence on the UV fluence is represented in Table 1. The tristimulus values *X*, *Y*, and *Z* decrease when raising the UV fluence to 120 kJ/cm^2, while the chromaticity coordinates *x* and *y* increased on raising the fluence to 120 kJ/cm^2. This was accompanied with a decrease in *z*.

The CIELAB intercept a^* shows the relation between red ($+a^*$) and green ($-a^*$), whilst the intercept b^* links the yellow ($+b^*$) and blue ($-b^*$). The L^* intercept correlate apparent lightness in CIELAB color space. The value of L^* is 100 for the ideal white and 0 for the ideal black. The precision in calculating L^* is ±0.05 and ±0.01 for both a^* and b^*, respectively. The fluence dependence of a^*, b^*, and L^* is represented in Figure 3. It is shown that both a^* and b^* displayed negative values that increased on raising the UV fluence to 120 kJ/cm^2. This indicates that the green and blue color components decrease and tends to be converted into red and yellow, respectively. This was associated with an increase in darkness in the NCP samples as indicated from the decrease in L^* with the UV fluence ($-L^*$) as seen in Figure 3.

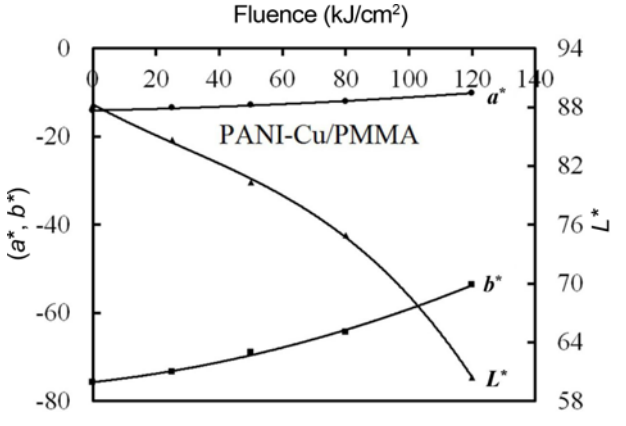

Figure 3. Variation of a^*, b^*, and L^* of PANI-Cu/PMMA NCP samples with the UV fluence.

Color Changes in the UV Irradiated PANI-Cu/CTA NCP Samples

The transmission spectra of the pristine and UV irradiated PANI-Cu/CTA, in the 370-780 nm range is shown in Figure 4. The *X*, *Y*, *Z* tristimulus values and *x*, *y*, *z* chromaticity coordinates were computed using the transmittance values, measured at the 370-780 nm range. The dependence of both *X*, *Y*, *Z* tristimulus values and *x*, *y*, *z* chromaticity coordinates on the UV fluence is represented in Table 1. The values indicated that *X*, *Y*, and *Z* show a similar trend to that of PANI-Cu/PMMA NCP samples, as they decreases when the UV fluence increases to 120 kJ/cm^2. The *x* and *y* coordinates increased on raising the fluence to 120 kJ/cm^2. This was accompanied with a decrease in *z*.

The dependence of a^*, b^*, and L^* on the UV fluence is represented in Figure 5. It is shown that both a^* and b^* displayed negative values that increased on raising the UV fluence to 120 kJ/cm^2. This indicates that the green and blue color components decreased. This was associated with an increase in darkness in the NCP samples as indicated from the decrease in L^* with the UV fluence as seen in Figure 5.

Color Changes in the UV Irradiated PANI-Cu/PC NCP Samples

The transmission spectra of the pristine and UV irradiated PANI-Cu/PC, in the 370-780 nm range is shown in Figure 6.

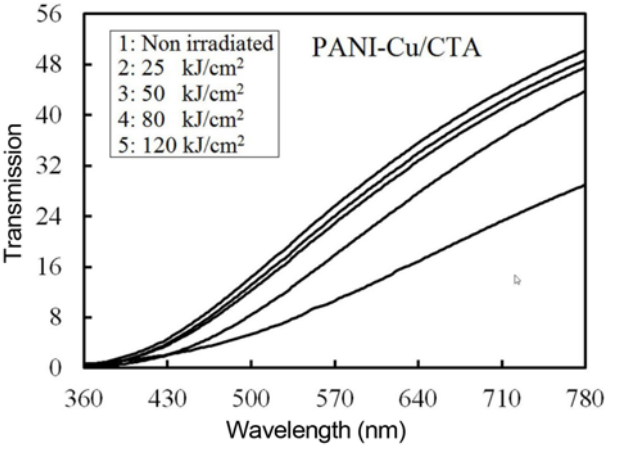

Figure 4. UV-Vis transmission spectra, in the 370-780 nm range, of the pristine and UV irradiated PANI-Cu/CTA NCP samples.

Table 1. Tristimulus values (*X*, *Y*, *Z*) and chromaticity coordinates (*x*, *y*, *z*) of the four synthesized NCPs as a function of UV fluence

Fluence (kJ/cm^2)	PANI-Cu/PMMA						Fluence (kJ/cm^2)	PANI-Cu/CTA					
	X	*Y*	*Z*	*x*	*y*	*z*		*X*	*Y*	*Z*	*x*	*y*	*z*
0	72.33	72.49	74.18	0.330	0.331	0.339	0	22.15	22.58	13.07	0.383	0.391	0.226
25	65.34	65.39	67.03	0.330	0.331	0.339	25	20.78	21.12	11.55	0.389	0.395	0.216
50	57.20	57.25	57.82	0.332	0.332	0.336	50	19.84	20.07	10.69	0.392	0.397	0.211
80	48.08	48.08	48.09	0.333	0.333	0.333	80	15.57	15.42	6.68	0.413	0.397	0.188
120	28.52	28.51	28.28	0.334	0.334	0.332	120	9.97	9.54	4.52	0.415	0.409	0.177
Fluence (kJ/cm^2)	PANI-Cu/PC						Fluence (kJ/cm^2)	PANI-Cu/PC-PBT					
	X	*Y*	*Z*	*x*	*y*	*z*		*X*	*Y*	*Z*	*x*	*y*	*z*
0	72.65	73.39	86.54	0.312	0.316	0.372	0	61.62	62.00	67.46	0.322	0.324	0.353
25	66.31	66.79	74.78	0.319	0.321	0.360	25	58.23	58.50	62.34	0.324	0.326	0.351
50	64.43	64.97	72.56	0.319	0.322	0.359	50	57.48	57.84	62.28	0.324	0.326	0.350
80	63.15	63.54	69.64	0.322	0.324	0.355	80	56.63	57.00	61.10	0.325	0.327	0.348
120	61.68	62.03	67.33	0.323	0.325	0.352	120	54.71	54.90	57.73	0.327	0.328	0.345

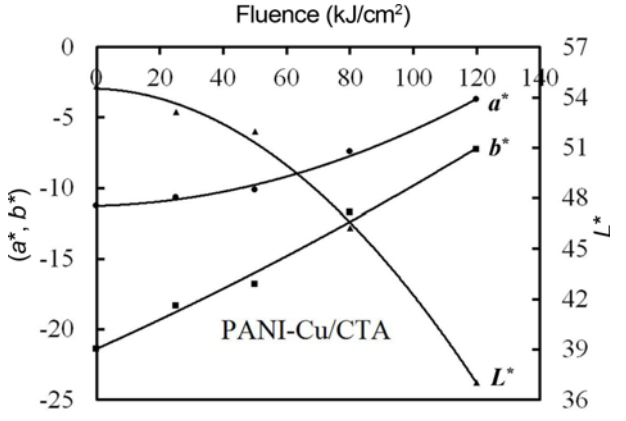

Figure 5. Variation of a^*, b^*, and L^* of PANI-Cu/CTA NCP samples with the UV fluence.

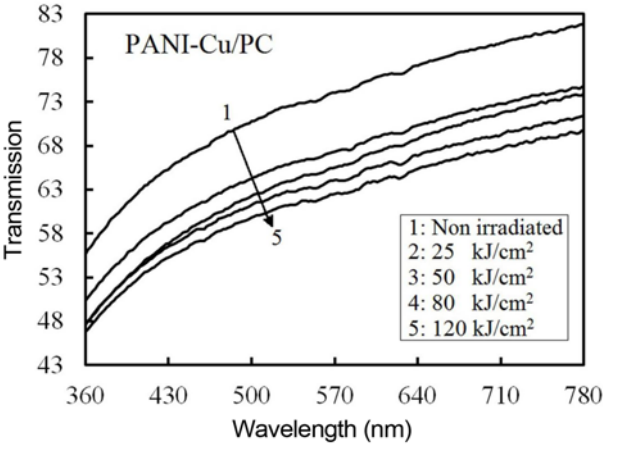

Figure 6. UV-Vis transmission spectra, in the 370-780 nm range, of the pristine and UV irradiated PANI-Cu/PC NCP samples.

The *X*, *Y*, *Z* tristimulus values and *x*, *y*, *z* chromaticity coordinates were computed using the transmittance values, measured at the 370-780 nm range. The dependence of both *X*, *Y*, *Z* and *x*, *y*, *z* on the UV fluence is represented in Table 1. The values indicated that *X*, *Y*, and *Z* exhibited a similar trend to that of PANI-Cu/PMMA and PANI-Cu/CTA NCP samples, as they decrease when the UV fluence increases to 120 kJ/cm^2. The *x* and *y* coordinates increased when the UV fluence increases to 120 kJ/cm^2. At the same time the *z* value decreased (Table 1).

The dependence of a^*, b^*, and L^* on the UV fluence is represented in Figure 7. It is shown that a^* is almost not affected by the UV fluences. The b^* intercept is slightly increased with increasing the fluence, which means that the yellow color component is slightly increased. At the same, the L^* decreased when the UV fluence increases, meaning an increase in darkness.

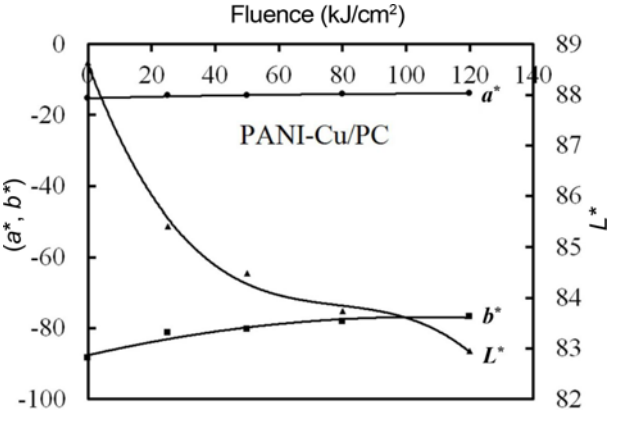

Figure 7. Variation of a^*, b^*, and L^* of PANI-Cu/PC NCP samples with the UV fluence.

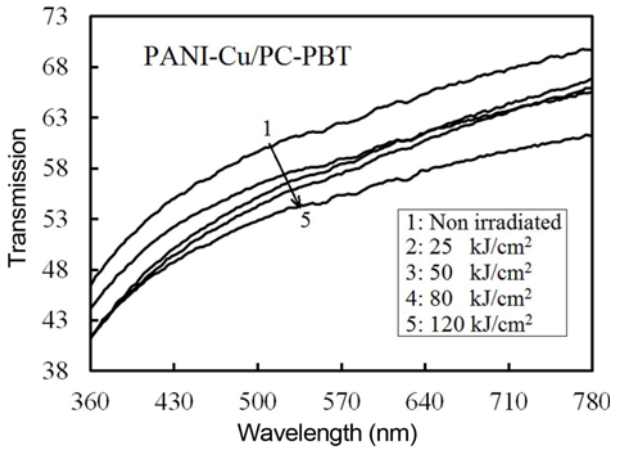

Figure 8. UV-Vis transmission spectra, in the 370-780 nm range, of the pristine and UV irradiated PANI-Cu/PC-PBT NCP samples.

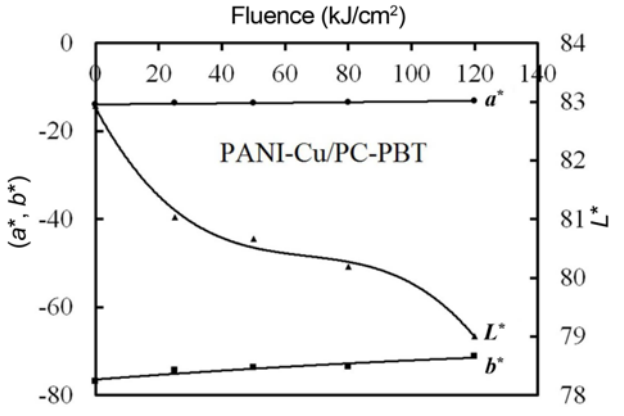

Figure 9. Variation of a^*, b^*, and L^* of PANI-Cu/PC-PBT NCP samples with the UV fluence.

Color Changes in the UV Irradiated PANI-Cu/PC-PBT NCP Samples

The transmission spectra of the pristine and UV irradiated PANI-Cu/PC-PBT, in the 370-780 nm range is shown in Figure 8. The *X*, *Y*, *Z* tristimulus values and *x*, *y*, *z* chromaticity coordinates were computed using the transmittance values, measured at the wavelength range 370-780 nm. The dependence of both tristimulus values and chromaticity coordinates on the UV fluence is represented in Table 1. The *X*, *Y*, and *Z* decreased when the UV fluence increased to 120 kJ/cm^2. The *x* and *y* coordinates increased with increasing the fluence to 120 kJ/cm^2. This was associated with a decrease in *z* values (Table 1).

The variation of a^*, b^*, and L^* with the UV fluence is represented in Figure 9. It is shown that a^* is not affected by the UV fluences. The b^* intercept is slightly increased when the fluence increased to 120 kJ/cm^2, indicating that the yellow color component is slightly increased. This was associated with an increase in the dark component of the NCP samples as indicated from the decrease in L^* with the UV fluence ($-L^*$) as seen in Figure 9.

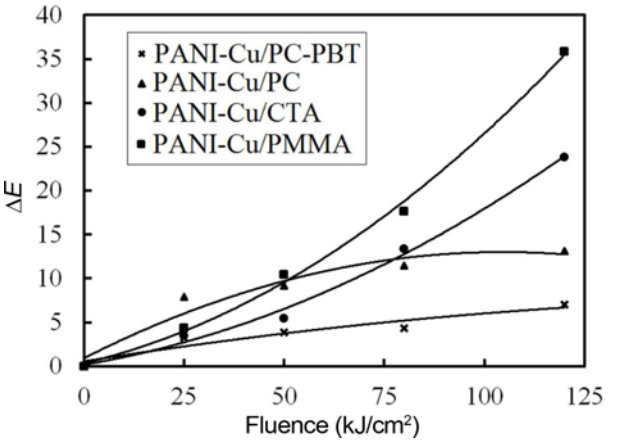

Figure 10. Variation of the color intensity (ΔE) of the four NCP systems with the UV fluence.

Color Differences between the Pristine and the Irradiated NCP Samples

The color intensity (ΔE) that denotes the color divergence between pristine and the irradiated NCP samples was computed for the four NCP systems by applying the CIELAB color difference equation [35] and is shown in Figure 10 vs. UV fluence. It is noticed that the values of ΔE for the PANI-Cu/PMMA NCP samples achieved a major color difference which is an acceptable match in commercial reproduction on printing presses since *E* reached the value of 35.8 [36,37]. The value of ΔE for the PANI-Cu/CTA NCP samples reached 23.8 that also indicates a significant color difference. On the other hand, the value of ΔE for the PANI-Cu/PC NCP samples shows an increase up to 13.1 which means lower color difference compared to that of PANI-Cu/PMMA and PANI-Cu/CTA NCPs. It is worth mentioning that the PANI-Cu/PC-PBT shows a minimum color difference since ΔE exhibited variation up to 7 (Figure 10). This means that the PANI-Cu/PC-PBT NCP samples have higher resistance to color changes against UV radiation. The color modifications are caused by the hot free radicals that are produced due to the UV radiation-induced break of the NCP molecules. Additionally, the hot free radicals that have electrons with unpaired spin, cause color variations [35]. On the other hand, the slight color variation of the PANI-Cu/PC-PBT can be due to the fact that the blend of PBT with PC enhances the compact structure of the PANI-Cu/PC-PBT NCP samples, allowing molecules to absorb energy of definite wavelengths in the UV range, mainly for the ester groups and the aromatic rings which are strong UV absorbers.

Conclusion

PANI-Cu/PMMA, PANI-Cu/CTA, PANI-Cu/PC, and PANI-Cu/PC-PBT nanocomposites were fabricated using both chemical oxidative and casting techniques. The induced alterations in the color of the synthesized NCPs owing to UV irradiation have been investigated.

Both the PANI-Cu/PMMA and PANI-Cu/CTA NCP samples have a high response to color alternation by UV irradiation since the values of ΔE achieved a significant color difference which is an acceptable match in commercial reproduction on printing presses.

The blend of PBT with PC created a more compact structure in the PANI-Cu/PC-PBT NCP samples, resulted in a good chemical resistance of the NCP to color changes, where it showed the least color difference. Thus, this NCP can be suitable candidate in textile industry to increase the resistance of the textile against color changes due to sunlight exposure.

References

1. T. J. Bixby, A. A. Cordones, and S. R. Leone, *Chem. Phys. Lett.*, **521**, 7 (2012).
2. A. S. Abdel-Naby and S. A. Nouh, *Polym. Degrad. Stab.*, **76**, 419 (2002).
3. S. A. Nouh, K. Benthami, A. M. Massoud, and N. T. El-Shamy, *Radiat. Eff. Defects Solids*, **173**, 956 (2018).
4. W. Zhao, Z. Wei, L. Zhang, X. Wu, and J. Jiang, *J. Alloys Compd*., **698**, 754 (2017).
5. K. Kamal, G. Nitendra, P. Singh, and R. Meera, *J. Phys. Conf. Ser.*, **365**, 012014 (2012).
6. P. K. Khanna, P. More, B. G. Bharate, and A. K. Vishwanath, *J. Lumin.*, **130**, 18 (2010).
7. X.-S. Jia, C.-C. Tang, X. Yan, G.-F. Yu, J.-T. Li, H.-D. Zhang, J.-J. Li, C.-Z. Gu, and Y.-Z. Long, *J. Nanomater.*, **2016**, 9102828 (2016).
8. B. Kim, V. Koncar, and C. Dufour, *J. Appl. Polym. Sci.*, **101**, 1252 (2006).
9. R. Huang, Y. Z. Long, C. C. Tang, and H. D. Zhang, *Adv. Mater. Res.*, **853**, 79 (2014).
10. N. Muthukumar, G. Thilagavathi, and T. Kannaian, *High Perform. Polym.*, **27**, 105 (2015).
11. Y. Zhang and G. C. Rutledge, *Macromolecules*, **45**, 4238 (2012).
12. F. Ahangaran, A. H. Navarchian, and F. Picchioni, *J. Appl. Polym. Sci.*, **136**, 48039 (2019).
13. M. Kumar, S. Arun, P. Upadhyaya, and G. Pugazhenthi, *Int. J. Mech. Mater. Eng.*, **10**, 7 (2015).
14. S. M. Khaled, R. Sui, P. A. Charpentier, and A. S. Rizkalla, *Langmuir*, **23**, 3988 (2007).
15. A. Lanata and E. P. Scilingo, "Smart Textiles: Technology and Wireless System Network Applications. Autonomous Sensor Networks", Springer, Berlin, Germany, 2012.
16. S. M. Ebrahim, A. B. Kashyout, and M. M. Soliman, *J. Polym. Res.*, **14**, 423 (2007).
17. A. J. M. Valente, H. D. Burrows, A. Y. Polishchuk, C. P. Domingues, O. M. F. Borges, M. E. S. Eusebio, T. M. R. Maria, V. M. M. Lobo, and A. P. Monkman, *Polymer*, **46**, 5918 (2005).
18. R. C. Law, *Macromol. Symp.*, **208**, 255 (2004).
19. S. A. Nouh, K. Benthami, R. M. Samy, and A. A. El-Hagg, *Chem. Phys. Lett.*, **741**, 137123 (2020).
20. C. Yi, Y. Yang, B. Liu, J. He, and Z. Nie, *Chem. Soc. Rev.*, **49**, 465 (2020).
21. T. Barot, D. Rawtani, and P. Kulkarni, *Heliyon*, **6**, e03601 (2020).
22. A. V. Firth, S. W. Haggata, P. K. Khanna, S. J. Williams, J. W. Allen, S. W. Magennis, I. D. Samuel, and D. J. Cole-Hamilton, *J. Lumin.*, **109**, 163 (2004).
23. S. A. Nouh, Y. E. Radwan, D. El fiky, M. M. Abutalib, R. A. Bahareth, T. M. Hegazy, and S. S. Fouad, *Radiat. Phys. Chem.*, **97**, 68 (2014).
24. T. Yamauchi, H. Nakai, Y. Somaki, and K. Oda, *Radiat. Meas.*, **36**, 99 (2003).
25. R. F. Khan, N. Ahmed, and M. Aslam, *Radiat. Meas.*, **33**, 129 (2001).
26. R. Mishra, S. P. Tripathy, D. Sinda, K. K. Dwivedi, S. Ghosh, D. T. Khathing, M. Muller, D. Fink, and W. H. Chung, *Nucl. Instrum. Methods*, **168**, 59 (2000).
27. H. M. Said, Z. I. Ali, and H. E. Ali, *J. Appl. Polym. Sci.*, **101**, 4358 (2006).
28. G. H. Angham, J. Khudheyer, A. Gamal, H. A. Mohammad, A. A. Ahmed, S. A. Dina, and Y. Emad, *Molecules*, **24**, 3557 (2019).
29. S. A. Nouh, M. H. Abdel-Kader, and M. B. Mohamed, *Adv. Polym. Tech.*, **36**, 21614 (2017).
30. R. Mishra, S. Tripathy, D. Fink, and K. Dwivedi, *Radiat. Meas.*, **40**, 754 (2005).
31. N. Elhalawany, A. R. Wassel, A. E. Abdelhamid, A. AbouElfadl, and S. A. Nouh, *J. Mater. Sci.: Mater. Electron.*, **31**, 5914 (2020).
32. N. Elhalawany, M. M. Saleeb, and M. K. Zahran, *J. Mater. Sci.: Mater. Electron.*, **28**, 18173 (2017).
33. S. A. Nouh, K. Benthami, and M. Abutalib, *Radiat. Eff. Defects Solids*, **171**, 135 (2016).
34. K. Nassau, "Color for Science, Art and Technology", Elsevier, New York, 1998.
35. S. A. Nouh, N. Gaballah, A. Abou Elfadl, and S. A. Alsharif, *Radiat. Prot. Dosim.*, **183**, 450 (2019).
36. R. F. Witzel, R. W. Burnham, and J. W. Onley, *J. Opt. Soc. Am.*, **63**, 615 (1973).
37. G. Wyszecki and G. H. Fielder, *J. Opt. Soc. Am.*, **61**, 1135 (1971).